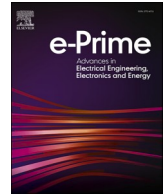


Contents lists available at [ScienceDirect](https://www.sciencedirect.com)

e-Prime - Advances in Electrical Engineering, Electronics and Energy

journal homepage: www.elsevier.com/locate/prime

Investigation of continuous pulse current source on the performance of phase change material-thermoelectric cooler system

Yanhong Guo^{a,b}, Xinyu Zhang^{a,b}, Jing Wang^{c,d}, Yuying Yan^e, Yong Ren^{a,b,c,f,*}^a Department of Mechanical, Materials and Manufacturing Engineering, University of Nottingham Ningbo China, Ningbo, China^b Research Group for Fluids and Thermal Engineering, University of Nottingham Ningbo China, Ningbo, China^c Nottingham Ningbo China Beacons of Excellence Research and Innovation Institute, Ningbo, China^d Department of Electrical and Electronic Engineering, University of Nottingham Ningbo China, Ningbo, China^e Research Group for Fluids and Thermal Engineering, University of Nottingham, Nottingham, UK^f Key Laboratory of Carbonaceous Wastes Processing and Process Intensification Research of Zhejiang Province, University of Nottingham Ningbo China, Ningbo, China

ARTICLE INFO

Keywords:

Thermoelectric cooler
Phase change material
Parameter study
Structural design

ABSTRACT

In this article, the influence of phase change materials (PCM) on the property of thermoelectric cooler (TEC) is studied by numerical simulation. The heat sink integrated with PCM is placed on the hot side of TEC to reduce the fluctuation of temperature under a continuous pulse current source. The performance of a single-layer PCM-TEC system with that of a single TEC system under continuous pulse current source is firstly compared. Based on this, the effects of current source type, PCM layer, pulse width, cooling load and pulse amplitude on the cooling performance of TEC are investigated in depth. The results show that, compared to a single TEC system, PCM is able to considerably enhance the cooling performance of the TEC during the phase transition period. Besides, increasing PCM layer or decreasing cooling load improves the phase change interval, which increases threefold when the cooling load increases from 0.02 W to 0.06 W. In addition, it is found that lower temperature can be achieved by increasing pulse width or pulse amplitude.

1. Introduction

The use of refrigerants in traditional refrigeration and air-conditioning systems poses a growing threat to the environment. In order to alleviate this problem, it is necessary to explore alternative cooling technologies without utilizing refrigerant. One of these technologies is the use of thermoelectric device for cooling purpose. Thermoelectric cooler (TEC) is an electronic device mainly made of semiconductor and its working principle is based on Thomson effect, Seebeck effect and Peltier effect to realize heat transfer without refrigerant [1]. Compared with other existing cooling technologies, it shows great advantages of no moving components, pollution-free, silent operation, light weight, easy control and easy adjustment. In addition, TEC has been used in industrial fields, space exploration and portable refrigerators [2]. Specially, it can be used in electronic chips to achieve point-to-point cooling [3]. The fundamental disadvantage of TEC is the low coefficient of performance (COP), which largely depends on the merit (ZT) for thermoelectric materials [4].

Although studies have been carried out to enhance the property of

thermoelectric materials [5–7], the thermoelectric materials developed cannot meet the industrial requirements due to their synthesis and other technical challenges. This obstacle has caused the imbalance between the development of device manufacturing and thermoelectric materials. Therefore, apart from studying the thermoelectric performance of materials, the structural optimization and thermal design technology of thermoelectric cooling system were also carried out [8–12]. Riffat and Qui [8] conducted experimental study on the performance of vapour compression (VCR) system and TEC system. The results showed that the COP of VCR system was much higher than that of TEC system. Hermes and Barbosa [9] presented a similar study and found that the efficiency of TEC system was 1% higher than that of VCR system. Gong et al. [10] investigated the impact of the TEC compact design on its various thermal mechanical properties and proved that the connection of thermal elements based on thicker ceramic plates contributed to better reliability and thermal stress distribution. Elghool et al. [11] summarized the potential ways to improve the design of heat sink for thermoelectric device, and reviewed the potential design structures of the heat sink for heat dissipation enhancement. Manikandan et al. [13] proposed a reversible thermodynamic system for TEC, and explored the influences of contact

* Corresponding author at: Department of Mechanical, Materials and Manufacturing Engineering, University of Nottingham Ningbo China, Ningbo, China.

E-mail address: yong.ren@nottingham.edu.cn (Y. Ren).

<https://doi.org/10.1016/j.prime.2023.100163>

Received 23 March 2023; Received in revised form 24 April 2023; Accepted 25 April 2023

Available online 29 April 2023

2772-6711/© 2023 The Authors. Published by Elsevier Ltd. This is an open access article under the CC BY-NC-ND license (<http://creativecommons.org/licenses/by-nc-nd/4.0/>).

Nomenclature		t	phase change temperature (K)
Abbreviation		u	velocity (m s^{-1})
COP	Coefficient of performance	V	voltage (V)
PCM	Phase change material	<i>Greek letters</i>	
TEC	Thermoelectric cooler	α	mass fraction
VCR	Vapour compression	θ	phase fraction
Symbols		ψ	electric potential (V)
A	convective heat transfer area (m^2)	ρ	density (kg m^{-3})
C_p	specific heat capacity ($\text{J kg}^{-1} \text{K}^{-1}$)	σ	electrical conductivity (S m^{-1})
E	electric field (V m^{-1})	Δ	Difference
J	electric current flux (A m^{-2})	<i>Subscript</i>	
h	convective heat transfer coefficient ($\text{W m}^{-2} \text{K}^{-1}$)	a	ambient
k	thermal conductivity ($\text{W m}^{-1} \text{K}^{-1}$)	C	cold side of TEC
L	latent heat capacity (J kg^{-1})	c	charge
P	peltier coefficient	H	hot side of TEC
Q	heat (W)	m	melting point
q	heat flux (W m^{-2})	1	solid state
S	seebeck coefficient	2	liquid state
T	temperature (K)		

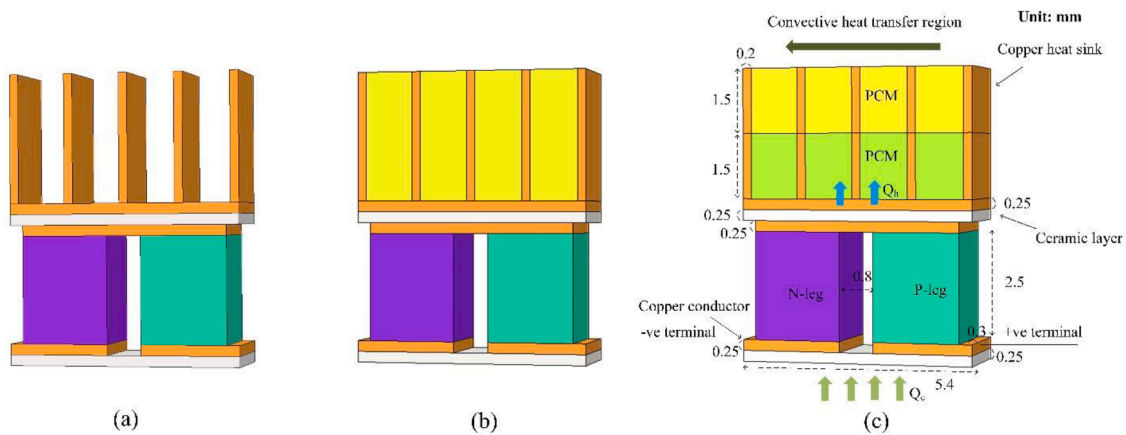


Fig. 1. Geometric Model of PCM-TEC: (a) Single TEC system; (b) Single-layer PCM-TEC system; (c) Double-layer PCM-TEC system.

Table 1
Material properties

Material	$C_p, \text{J/kg K}$	$\rho, \text{kg m}^{-3}$	$S, \text{V K}^{-1}$	$\sigma, \text{S m}^{-1}$	$k, \text{W m}^{-1} \text{K}^{-1}$
Ceramics	850	3960	-	-	18
Bismuth telluride	154	7700	$(22224 + 930.6T - 0.9905T^2) \times 10^{-9}$	$1/(5112 + 163.4T + 0.6279T^2) \times 10^{-10}$	$(62605 - 277.7T + 0.4131T^2) \times 10^{-4}$
Copper	385	8960	-	-	400

Table 2
PCM properties

PCM	T_m, K	$\rho, \text{kg m}^{-3}$	$L, \text{J kg}^{-1}$	$C_p, \text{J kg}^{-1} \text{K}^{-1}$	$k, \text{W m}^{-1} \text{K}^{-1}$
OP28E [30]	301.15	880 (solid)	244000	1934 (solid)	0.358 (solid)
		770 (liquid)		2196 (liquid)	0.148 (liquid)
OM32[19]	308.15	915 (solid)	191000	3200 (solid)	0.25 (solid)
		880 (liquid)		2800 (liquid)	0.125 (liquid)

Table 3
Boundary condition.

	Equation	Location
Heat input	$Q_c = \text{constant}$	The cold side of TEC
Convection	$Q = hA(T - T_a)$	Top side of heat sink

resistance, annual shape and temperature ratio on the energy/exergy efficiency and cooling power of the TEC. The results showed that the cooling performance of TEC was obviously affected by contact resistance. Wang et al. [14] explored the effects of structural factors on the property of TEC. Results showed that the cooling power of the optimal TEC could be improved by 43.83% when the temperature variation

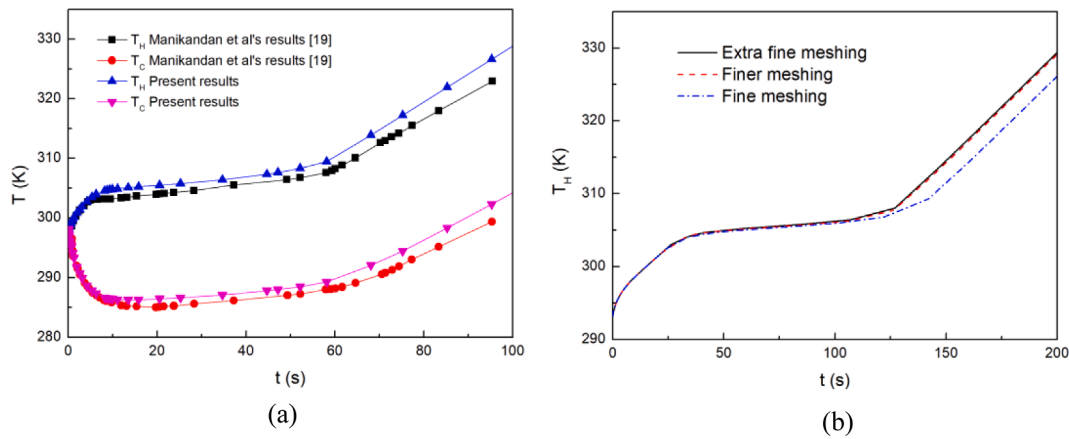


Fig. 2. (a) Transient temperature variation of the hot and cold sides of the TEC; (b) Transient temperature variation of the hot side of the TEC.

Table 4
Number of elements and nodes in different meshing.

	Fine meshing	Finer meshing	Extra fine meshing
Nodes	1875	4056	14585
Elements	8469	19625	77495

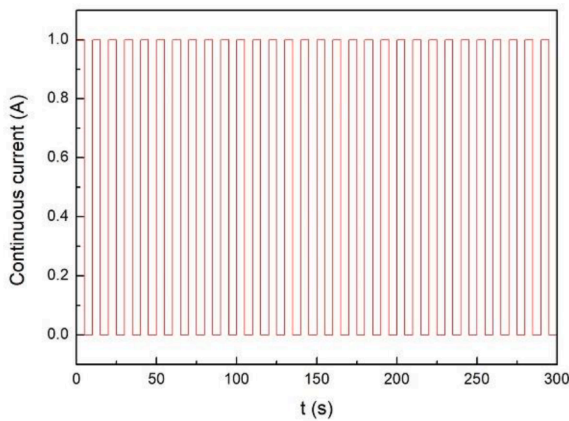


Fig. 3. Continuous pulse current source.

Table 5
Baseline condition for parameters

Type of PCM	Pulse width	Pulse amplitude	Cooling load
OM32	5 s	1 A	0.02 W

between two sides of TEC reached 60 K. Manikandan and Kaushik [15] simulated TEG and TECs with annular geometry to improve their energy conversion efficiency. The results showed that the COP of thermoelectric device could be increased when the surface area of the hot side increased. Based on above researches, the geometry structure and the design the heat sink have a huge impact on the property of TEC.

On the other hand, Phase change material (PCM) has unique properties, such as high latent heat, thermal stability, chemical stability, non-corrosivity and high reliability [16]. The feasibility of using PCM for thermal management of electronic equipment has been explored. Tan and Zhao [17] investigated the PCM-TEC system for space cooling. Results showed that the property of TEC could be obviously increased by using PCM. Li et al. [18] discussed the effect of TEC with PCM for multiple sclerosis patients. It was found that the temperature of TEC was

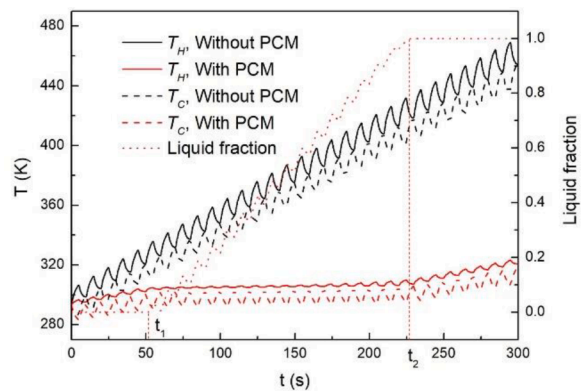


Fig. 4. Variation of temperature in the hot (T_H) and cold (T_C) sides of the TEC and liquid fraction of PCM.

kept the temperature of 10°C for 1200 s by using PCM. Manikandan et al. [19] conducted a numerical study on the thermal property of the TEC combined with PCM. It was found that under the condition of 0.03 W heat load and heat transfer coefficient as $5 \text{ W m}^{-2} \text{ K}^{-1}$, the cold and hot end temperatures of PCM could be, respectively, decreased to 13°C and 22°C. Wang et al. [20] discussed the performance of PCM-TEC system for aerospace application and found that the required temperature of TEC could be controlled and the COP was more than two times the case of without PCM. It should be noted that most of the current researches [21–24] on the performance of PCM-TEC system are under condition of constant current source. However, when the pulse current is employed to the TEC, the cold end temperature instantly decreases due to Peltier cooling and then rises to a peak point and achieves peak overshoot based on the accumulation of Joule heat in the thermos-element and Fourier heat conduction through the thermos-elements from the hot side to the cold side of the TEC. Researches on the pulse current cooling effect have been carried out to achieve a lower temperature in a single TEC system by using a current pulse input source [25–28]. This is the transient supercooling phenomenon [29]. However, few studies focused on the cooling property of the PCM-TEC system under the continuous pulse current source.

It was found from the literature survey that the use of PCM can affect the temperature of TEC, thereby improving its performance. In addition, using continuous current pulse in the TEC system can achieve lower temperatures. Based on these, a computational study of the TEC system with a heat sink integrated with PCM under a continuous current pulse source has been carried out. The influence of the presence of PCM on the performance of TEC has been considered. The impact of current pulse type, PCM layer, cooling load, pulse amplitude, and pulse width on TEC

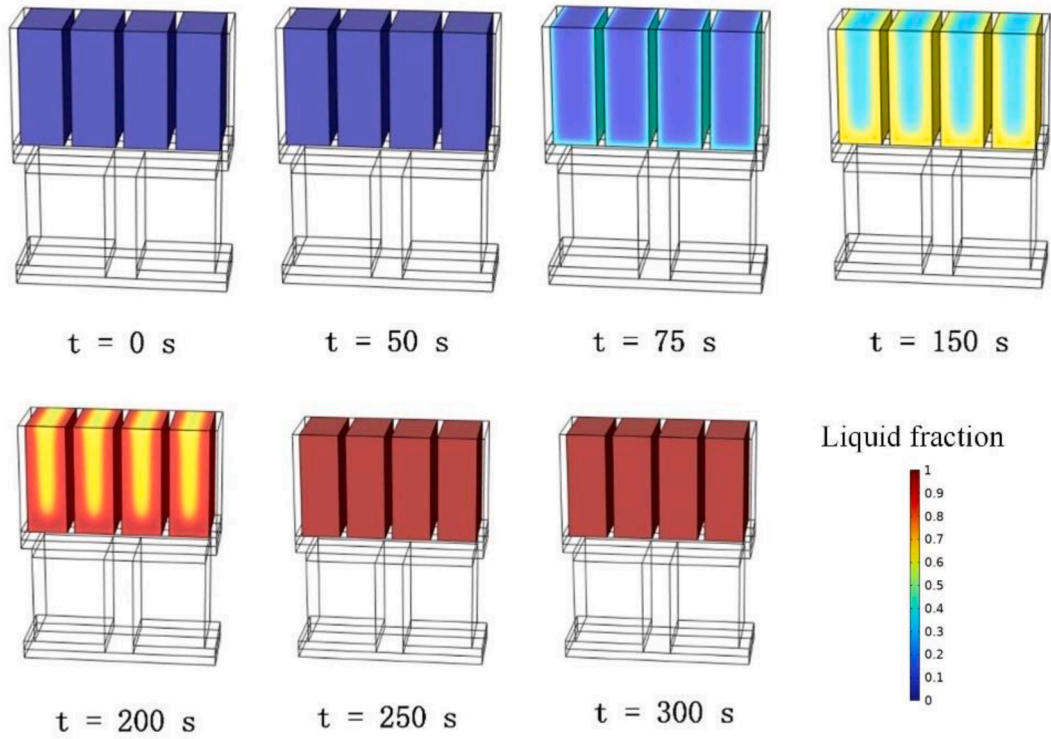


Fig. 5. Variation of liquid fraction in single-layer PCM-TEC system.

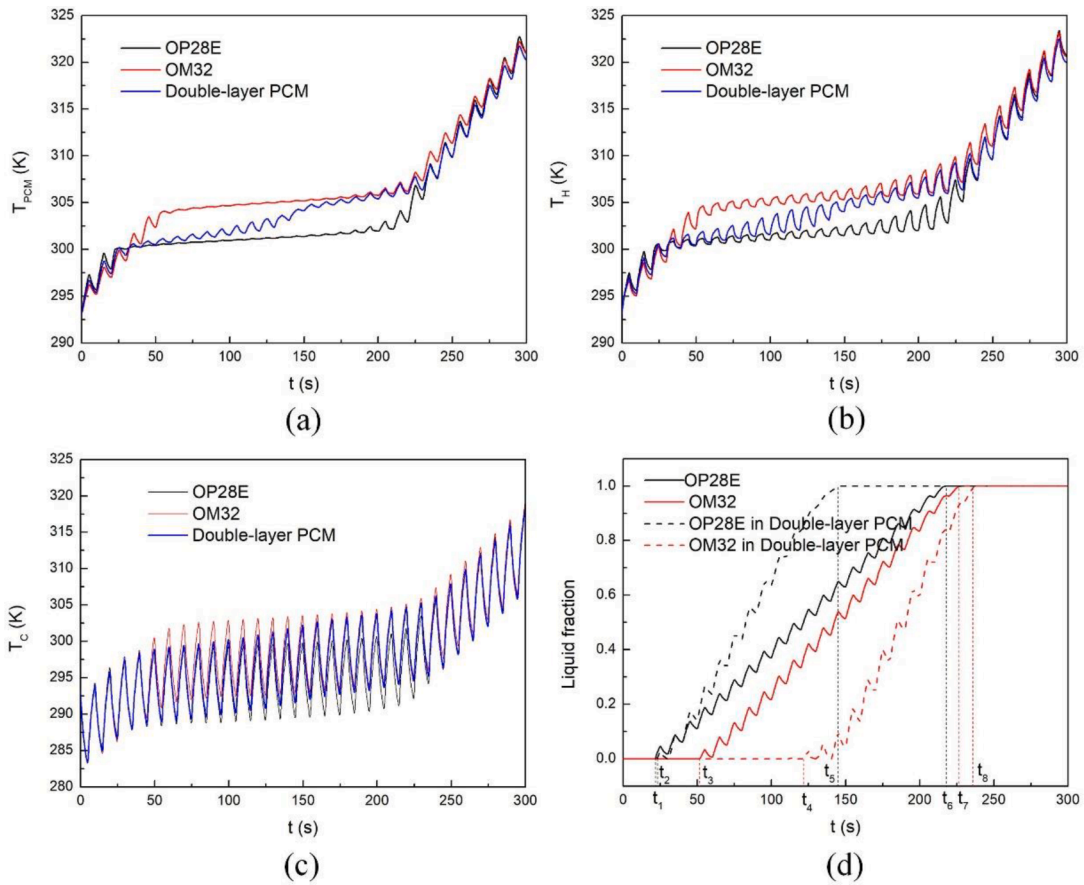


Fig. 6. (a) Transient variation of PCM temperature; (b) Transient variation of TEC temperature in the hot side; (c) Transient variation of TEC temperature in the cold side; (d) Transient variation of liquid fraction.

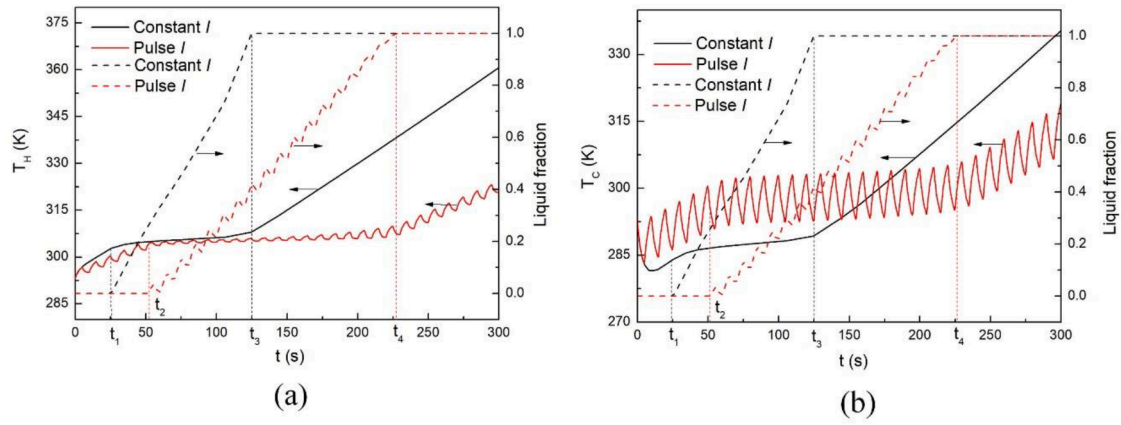


Fig. 7. (a) Transient variation of TEC temperature in the hot side and the liquid fraction of PCM; (b) Transient variation of TEC temperature in cold side and the liquid fraction of PCM.

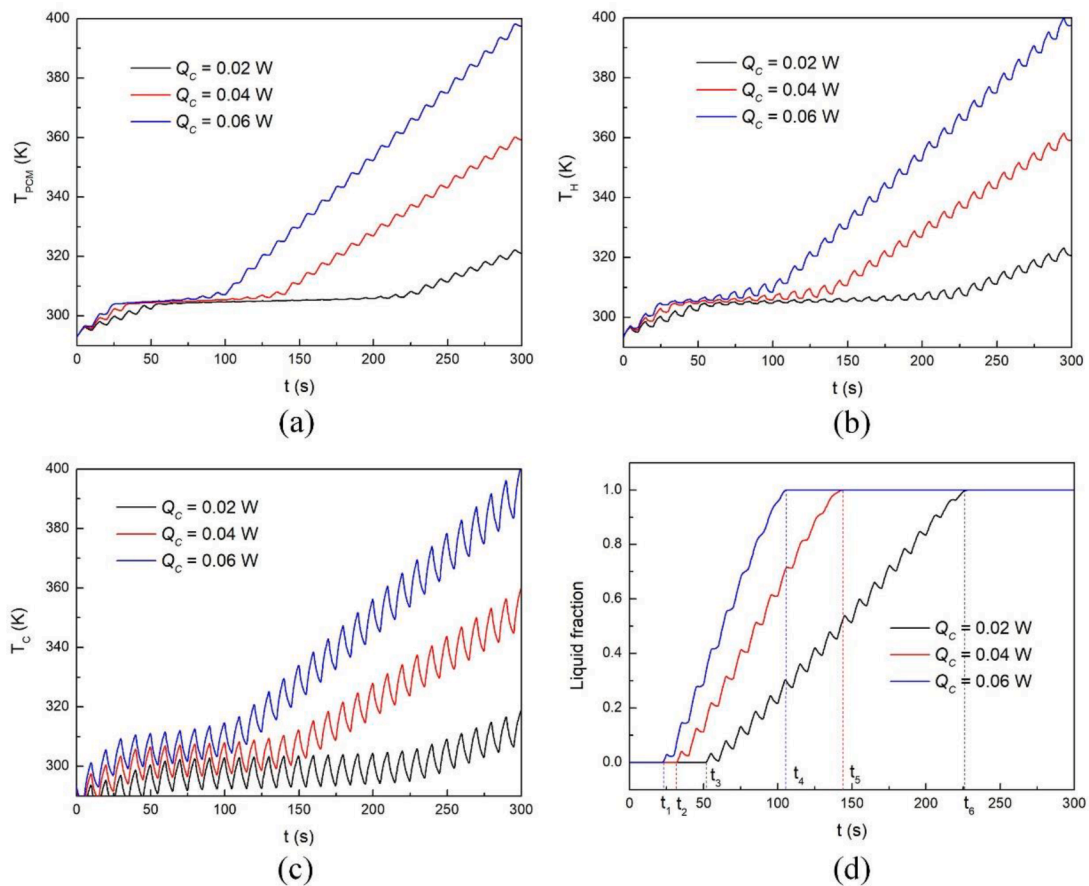


Fig. 8. (a) Transient variation of PCM temperature; (b) Transient variation of temperature in the hot side of the TEC; (c) Transient variation of temperature in the cold side of the TEC; (d) Transient variation of liquid fraction.

thermal management has also been analyzed.

2. Numerical method

A TEC module normally contains tens to hundreds of TEG units, due to the periodic arrangement of TEC units, this paper selects TEC unit instead of TEC module for modeling. As seen from Fig. 1, TEC unit normally consists of two insulating ceramic plates, three metal-based connectors, one P-type and one N-type thermal leg. In this study, OM32 and OP28E have been used as PCM, which are filled in the heat

sink. Single-layer or double-layer heat sink filled with PCM is placed on the hot side of TEC, i.e. single-layer PCM-TEC system in Fig.1 (b), and double-layer PCM-TEC system in Fig. 1 (c). Bi_2Te_3 is used as semiconductor material, Al_2O_3 is used as ceramic material, and Cu is selected as connector material. Table 1 lists the relevant material properties.

2.1. Selection of PCM

The choice of PCM depends on its thermal-physical properties, chemical stability, availability, stability and cost. In this study, PCM

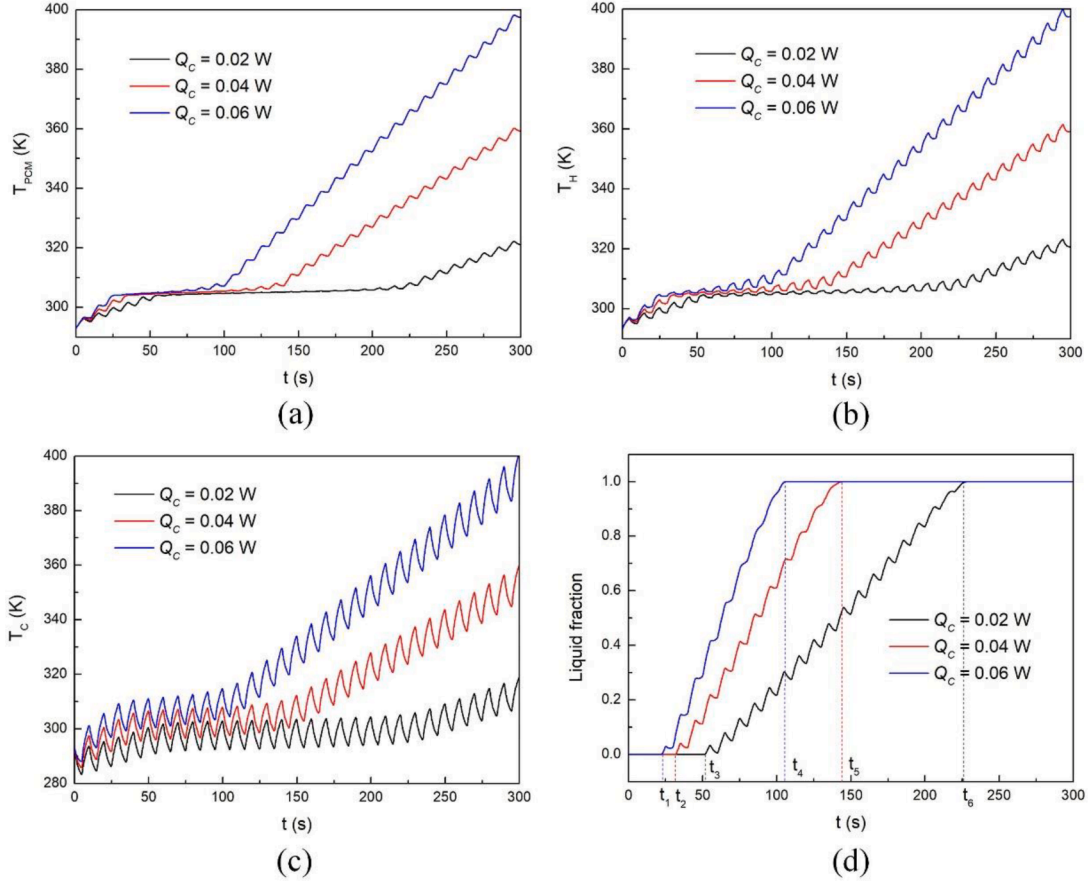


Fig. 9. (a) Transient variation of PCM temperature; (b) Transient variation of temperature in the hot side of TEC; (c) Transient variation of temperature in the cold side of TEC; (d) Transient variation of liquid fraction.

should be chosen in such a way that its melting point is slightly higher than the environment temperature, thus it will not melt under ambient temperature, but it should undergo phase change transition when reaching to the temperature of the hot side of the TEC. Therefore, OP28E [30] and OM32 [19] with melting points of 301.15K and 305.15K respectively are selected as the PCMs studied in this paper. The properties of the PCMs are listed in Table 2.

2.2. Governing equations and boundary conditions

The PCM-TEC system developed in this study contains heat transfer equation and electric potential equation. The coupling energy and potential control equations can be written as:

$$\rho C_p \frac{\partial T}{\partial t} + \nabla \cdot q = Q \quad (1)$$

$$\frac{\partial \rho_c}{\partial t} + \nabla \cdot J = 0 \quad (2)$$

where ρ is the density and C_p is specific heat capacity; q is the heat flux generated by Peltier effect and Fourier effect; Q is the Joule heat; J and ρ_c are, respectively, the current density and the charge density.

The relationship between heat flux, electric field and current density can be given by:

$$q = PJ - k\nabla T \quad (3)$$

$$Q = JE \quad (4)$$

where P and E are, respectively, the Peltier coefficient and electric field, which are realized in the following ways:

$$P = ST \quad (5)$$

$$E = -\nabla\psi + S\nabla T \quad (6)$$

where S and ψ are, respectively, the seebeck coefficient and electrical potential. The J is solved by:

$$J = \sigma E \quad (7)$$

In PCM, the phase change process is characterized by the following energy equation:

$$PC_p \frac{\partial T}{\partial t} = \nabla \cdot (k\nabla T) + Q' \quad (8)$$

where Q' refers to internal heat generation, C_p is expressed as:

$$C_p = \frac{1}{\rho} (\theta_1 \rho_1 C_{p,1} + \theta_2 \rho_2 C_{p,2}) + L_{1 \rightarrow 2} \frac{\partial \alpha}{\partial T} \quad (9)$$

where subscripts 1 and 2, respectively, refer to solid and liquid phase. The introduced latent heat L is additional term supposing the phase change occurs between $(T_m - \frac{\Delta T_m}{2})$ and $(T_m + \frac{\Delta T_m}{2})$. In the calculation process within the phase change range, the phase change function θ_1 and θ_2 quantitative calculation by temperature is defined as:

$$\theta_1 = 1, \theta_2 = 0, T < T_m - \frac{\Delta T_m}{2} \quad (10)$$

$$\theta_1 = \frac{(T_m + \frac{\Delta T_m}{2}) - T}{\Delta T_m}, \theta_2 = \frac{T - (T_m - \frac{\Delta T_m}{2})}{\Delta T_m}, \text{ if } T_m - \frac{\Delta T_m}{2} < T < T_m + \frac{\Delta T_m}{2} \quad (11)$$

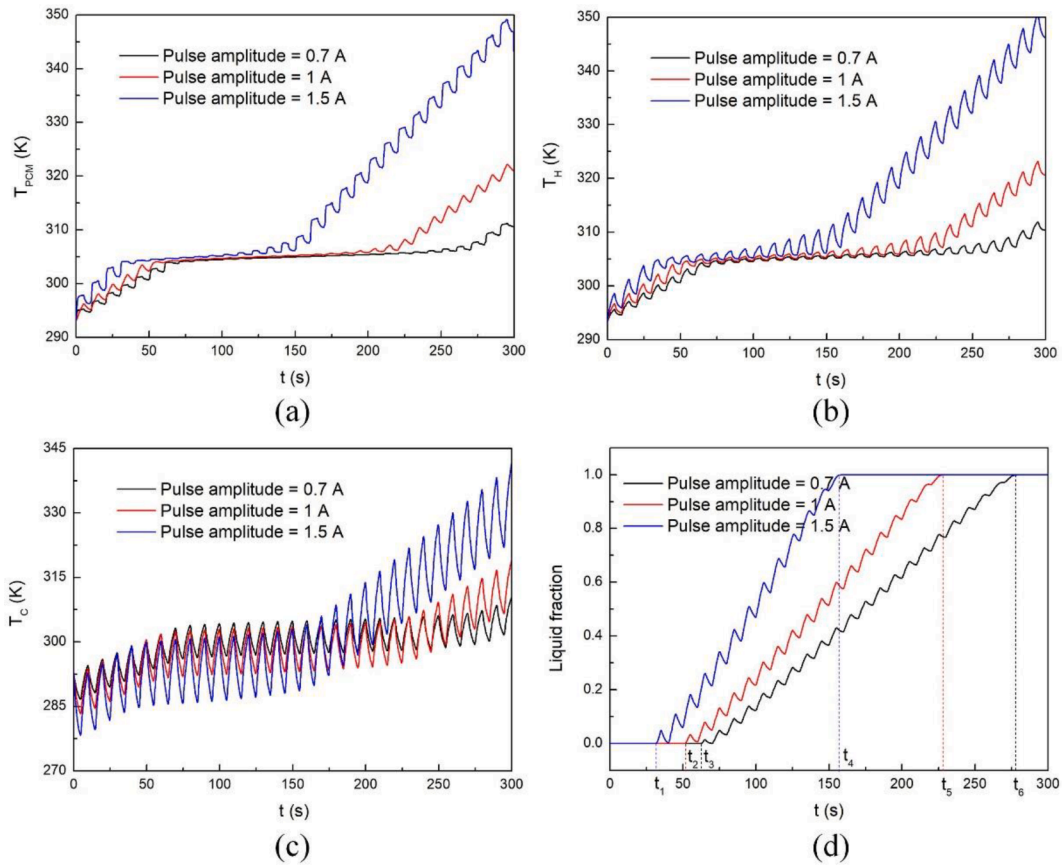


Fig. 10. (a) Transient variation of PCM temperature; (b) Transient variation of temperature in the hot side of TEC; (c) Transient variation of temperature in the cold side of TEC; (d) Transient variation of liquid fraction.

$$\theta_1 = 0, \theta_2 = 1, T > T_m - \frac{\Delta T_m}{2} \quad (12)$$

where, T_m is the melting point of PCM, ΔT_m is the temperature region of phase change, which is equal to 3 K in this study.

The smooth function of mass fraction, α , can be calculated based on the density before and after the phase change process, $\alpha = -1/2$ before the phase change and $\alpha = 1/2$ after the phase change, and it increases with the phase change develops, mass fraction α is expressed by equation (13):

$$\alpha = \frac{1}{2} \frac{\theta_2 \rho_2 - \theta_1 \rho_1}{\theta_1 \rho_1 + \theta_2 \rho_2} \quad (13)$$

$$\rho = \theta_1 \rho_1 + \theta_2 \rho_2 \quad (14)$$

The heat conductivity can be expressed as:

$$k = \theta_1 k_1 + \theta_2 k_2 \quad (15)$$

In this study, the initial temperature is 293.15 K. The boundary condition can be found in Table 3.

2.3. Numerical treatment

Comsol Multiphysics is used to solve the nonlinear temperature and electric field equations to realize the transient coupling solution of TEC-PCM system. The first-order scheme is used to integrate time with the introduced coupling equations and those nonlinear resolutions are achieved through the PARDISO solver. Set the relative tolerance as a parameter to check convergence. Particularly, the relative tolerance specified is 10^{-2} . The time step adopts BDF (backward differentiation formula). The initial simulation time step is set to 10^{-3} s, and the time

step can be freely changed, with a maximum value of 0.05 s. In this way, the software itself can automatically maximize the time step size, thereby reducing the computational workload of problem-solving. 4 cores is used in parallel by the COMSOL Multiphysics process. The simulations are conducted by using a workstation equipped with an Intel (R) Core(TM) i7-10510U CPU 1.80 GHz processor and 32 GB and 2667 MHz RAM.

The calculation model in this paper is based on the following assumptions:

- a) 3D transient heat conduction
- b) Ignore electrical contact resistance and thermal contact resistance
- c) Thermoelectric performance is temperature dependent

3. CFD code validation

In order to verify the simulation results of this study, the same geometric model, material properties and test conditions are chosen as Manikandan [23] et al. for numerical calculation. Fig. 2 (a) shows the hot and cold side temperature of TEC under the condition of current, cooling load and heat transfer coefficient are, respectively, 1 A, 0.03 W and $5 \text{ W m}^{-2} \text{ K}^{-1}$. It can be observed the predicted values are very similar to the published data [23], which illustrates that the numerical model proposed in this study is feasible. Besides. Grid independence verification is also carried out to make sure the simulation results do not rely on grid size. This study selects the physical field control grid, which means COMSOL will automatically divide the grid based on the settings of the physical field in the model. Fig. 2 (b) gives the temperature profile of the hot side of the TEC in single-layer PCM-TEC system under different grid conditions. It can be seen that the curves under the finer meshing grid and extra fine grid are basically coincident with each

other. Therefore, in order to save the calculation cost, this paper chooses the finer meshing grid for simulation and its specifications are listed in Table 4.

4. Results and discussion

Because PCM normally has low thermal conductivity, which will reduce the thermal diffusion process when it is directly connected to the TEC. Therefore, this paper employs the combination of fins and PCM to improve the heat transfer process. Heat can be diffused rapidly inside its volume due to the high thermal conductivity of heat sink made of copper. In order to evaluate the applicability of PCM-TEC system under the continuous pulse current source as shown in Fig. 3, the performance of PCM-TEC system with that of a single TEC system is firstly compared. After that, the influences of different type of PCM and different layers of PCM on the properties of TEC are investigated. Finally, the effects of current source type, pulse width, cooling load and pulse amplitude on the cooling property of TEC are evaluated in depth. The baseline condition in this study is shown in Table 5.

4.1. Performance of TEC with or without PCM

In this section, the impacts of PCM on the performance of TEC is discussed. All parameters are consistent with baseline situation. Fig. 4 gives the profile of the PCM liquid fraction and the temperature of the cold (T_H) and hot (T_c) sides of the TEC under continuous pulse current. It can be seen that both T_H and T_c of the PCM-TEC system are considerably lower than that of the single TEC system. The T_c reaches about 454 K in the single TEC system at $t = 300$ s, which is much higher than that of in the PCM-TEC system, which is 318 K, indicating that PCM can greatly improve the cooling performance of the TEC. It is worth noted that during the phase transition interval (from t_1 to t_2) period, the T_H and T_c basically fluctuates in a balanced position, which is because PCM absorbs lots of latent heat during the phase transition process and the temperature of PCM remains basically unchanged, thereby reducing the rising speed of the TEC. Similarly, Fig. 5 shows a 3D view of the PCM liquid fraction in the heat sink. The liquid fraction remains zero before $t = 50$ s, then gradually increased to one before $t = 250$ s, indicating a complete melting of the PCM, which is consistent with that of in Fig. 4. Based on above analysis, it can be concluded that the PCM enables to significantly enhance the performance of TEC especially in the phase change period.

4.2. Impact of PCM layer on TEC performance

In this part, the impacts of PCM layer on the performance of TEC is discussed. All parameters are consistent with the baseline situation. Fig. 6 gives the changes of T_{PCM} , T_H , T_c and liquid fraction of PCM under three different PCM-TEC systems, where the heat sink are, respectively, filled by OP28E, OM32 and both of OP28E and OM32 (OP28E is place in the upper layer, OM32 is placed in the lower layer). As can be seen in Fig. 6, the T_{PCM} , T_H and T_c in the single layer PCM-TEC systems increase rapidly in the non-phase change region, and remain basically unchanged during phase change period. Meanwhile, the values of T_{PCM} , T_H and T_c in the two-layer PCM-TEC system are always between that of the single layer OP28E-TEC system and single layer OM32-TEC system during phase change period, and exhibits a significant upward trend compared to the other two single layer PCM-TEC systems. This is because in the double-layer PCM-TEC system, there is only OP28E which changes from solid to liquid during t_2 to t_4 period, thus leads to its temperature close to that of OP28E-TEC system, while in the period of t_5 to t_8 , there is only OM32 undergoes phase change period, thus leads to its temperature close to that of OM32-TEC system, and in the t_4 to t_5 period, both OP28E and OM32 undergo phase transformation, which lead to the T_{PCM} , T_H and T_c of the double layer PCM-TEC system is basically equal to the average of the corresponding temperatures in the two single-layer

systems. In addition, the liquid fraction of the three systems rises regularly during phase transition period under continuous pulse current. In the single layer PCM-TEC systems, OP28E melts earlier than OM32, i. e. $t_3 > t_2$, which is due to OP28E has a lower melting point than OM32. Meanwhile, the OP28E in the single layer PCM-TEC system basically melts at the same time as the double layer PCM-TEC system, i. e. $t_1 \approx t_2$, which is because the double layer PCM-TEC system also contains OP28E in the heat sink. It is worth noted that the phase transition interval in the two-layer PCM-TEC system is larger than that of the other two single-layer PCM-TEC systems, i. e. $t_8 - t_2 > t_6 - t_1$ and $t_8 - t_2 > t_7 - t_3$, which means that the double-layer PCM can keep the TEC at a lower temperature for a longer period of time than the single-layer PCM, and further make the T_H and T_c lower than the single-layer PCM-TEC systems after the phase transition, as seen from Fig.6 (b,c).

4.3. Impact of pulse type

In this section, the effects of different types of current sources (constant current and continuous pulse current) on PCM-TEC system will be investigated. Fig. 7 shows that PCM first undergoes a phase transition under a constant current input, i. e. $t_1 > t_2$, indicating that PCM absorbs heat at a faster rate, thereby reaching the phase transition temperature earlier than that of under a continuous pulse current input. In addition, the phase transition interval of PCM under a continuous pulse current source is basically 1.75 times greater than that of under a constant current source, i. e. $t_4 - t_1 > 1.75(t_3 - t_2)$. From t_1 to t_3 , T_H and T_c remain basically unchanged under a constant current source, while they exhibit periodic fluctuations under a continuous pulse current source. Besides, during this time period, the T_H under the constant current is slightly higher than that of under continuous pulse current source, while T_c is much lower than the latter, which indicates that a constant current source makes better cooling effects for TEC during this time period. From t_3 to t_4 , the PCM is in a completely melting state under a constant current source while the phase transition process is still occurring under a continuous pulse current source. Therefore, during this time period, T_H and T_c rapidly rise in the former case, while maintaining periodic changes in the latter case, which leads to the T_c under the constant current source is first smaller than that of under the continuous pulse current source, and then exceeds the former during t_3 to t_4 period. Meanwhile, the T_H under the constant current source become much higher than that of under continuous current source during t_3 to t_4 period, which may lead the TEC device failure in this high operating temperature [31]. Based on the above analysis, it can be concluded that the PCM has better cooling effects for TEC during t_3 to t_4 period under the continuous pulse current source than that of under constant current source.

4.4. Impact of cooling load

The effects of cooling loads on the T_{PCM} , T_H , T_c and the liquid fraction of PCM under the continuous pulse current source are studied in this part. All other parameters are consistent with the baseline conditions except for the cooling load. As shown in Fig. 8, under continuous pulse current source, T_c first decreases to the lowest point, then gradually rises to its maximum point continuously, which is the transient supercooling phenomenon. After that, the T_c remains basically unchanged, and finally gradually rises to a stable fluctuation state. In addition, as the cooling load increases, the T_c increases, and a higher minimum temperature is obtained. Meanwhile, the T_{PCM} and T_H increase faster under lower cooling load, which is because of the higher cooling load speeded up the process of PCM melting under higher cooling load. As can be clearly seen in Fig. 8, for $Q_C = 0.02$ W, it takes 250 s to achieve complete melting, which is 2 times greater than that of when $Q_C = 0.06$ W. Therefore, it can be found from above analysis that the phase transition interval decreases with the increases of cooling load, and the PCM effectively improves the performance of TEC under a lower cooling load in the phase

transition period.

4.5. Impact of the pulse width

In this section, the influence of pulse width on the thermal behaviors of PCM-TEC system is studied. All other conditions are consistent with the baseline situation except for pulse width. Fig. 9 gives the increase of pulse width basically does not affect the growth rate of T_{PCM} , T_H and T_c , but the greater the pulse width, the greater of their fluctuation. Besides, the T_c with a higher pulse width achieves a lower minimum temperature. This is due to the increase of pulse width barely affect the phase change speed of PCM filled in the heat sink as given in Fig. 9 (d), but a higher pulse width means a longer time of the continuous current input for the first current pulse, which makes TEC achieve a lower minimum temperature.

4.6. Impact of the pulse amplitude

In this part, the effects of pulse amplitude on the changes of T_{PCM} , T_H , T_c and the liquid fraction of PCM are studied. All other conditions are consistent with the baseline values except for the pulse amplitude. Fig. 10 shows that the T_{PCM} and T_H increase and the minimum T_c decreases with the increasing pulse amplitude, which is due to the increase of pulse amplitude causes rapid phase change of PCM, and also, the TEC achieves a lower minimum temperature when the pulse amplitude is higher. As shown in Fig. 10 (d), it takes 280 s to achieve complete melting of the PCM when the pulse amplitude is 0.7 A, while it only requires 160 s for that of when amplitude equals to 1.5 A. Therefore, it can be found from above analysis that although increasing the amplitude achieves a lower cooling temperature for the TEC, it also reduces the time interval for the TEC to maintain the low temperature.

5. Conclusion

In order to improve the cooling performance of TEC under the condition of a continuous current source, a PCM-TEC system is established and the performance of the proposed system is evaluated. The main conclusions are as follows:

- Compared to a single TEC system, PCM can significantly improve the cooling performance of the TEC in the phase transition period.
- The temperature of PCM and the temperature of the cold and hot sides of TEC in the double-layer PCM-TEC system are always between that of in single layer OP28E-TEC system and single layer OM32-TEC system during phase change period, and exhibits a significant upward trend compared to the other two single layer PCM-TEC systems.
- The temperature of the cold side of TEC under continuous pulse current input is lower than of under constant current source during phase change period.
- When the cooling load is 0.02 W, the phase transition time of the PCM-TEC system is 3 times that of when the cooling load is 0.06 W, and the PCM effectively improves the performance of TEC at a lower cooling load in the period of phase change.
- The increase of pulse width barely influences the growth rate of the temperature of PCM and both sides of TEC, but enhances their fluctuation. Besides, the cold side of TEC with a higher pulse width achieves a lower minimum temperature.
- The increase of the pulse amplitude results in a lower cooling temperature for the TEC. Meanwhile, it also reduces the time interval for the TEC to maintain a low temperature.

Declaration of Competing Interest

The authors declare that they have no known competing financial interests or personal relationships that could have appeared to influence

the work reported in this paper.

Data availability

Data will be made available on request.

Acknowledgment

This work was financially supported by Zhejiang Natural Science Foundation under project code LY18E060004 as well as the Zhejiang Provincial Key Laboratory for Carbonaceous Wastes Processing and Process Intensification Research funded by the Zhejiang Provincial Department of Science and Technology (2020E10018). The authors also acknowledge the financial support from Nottingham Ningbo China Beacons of Excellence Research and Innovation Institute.

Supplementary materials

Supplementary material associated with this article can be found, in the online version, at doi:10.1016/j.prime.2023.100163.

References

- [1] T. Guclu, E. Cuce, Thermoelectric coolers (TECs): from theory to practice, *J. Electron. Mater.* 48 (1) (2019) 211–230.
- [2] A. Rezaia, L.A. Rosendahl, H. Yin, Parametric optimization of thermoelectric elements footprint for maximum power generation, *J. Power Sources* 255 (2014) 151–156.
- [3] M. Waldrop, The chips are down for Moore's law, *Nat. News* 530 (2016) 144.
- [4] S.B. Riffat, X. Ma, Improving the coefficient of performance of thermoelectric cooling systems: a review, *Int. J. Energy Res.* 28 (9) (2004) 753–768.
- [5] J. He, T.M. Tritt, Advances in thermoelectric materials research: looking back and moving forward, *Science* 357 (6358) (2017) 9997.
- [6] T.T. Lam, W.K. Yeung, Material property effect on conical semiconductor element temperatures in inhomogeneous thermoelectric coolers, *Int. Commun. Heat Mass Transf.* 117 (2020), 104743.
- [7] J. Zhang, X. Song, X. Zhang, Q. Zhang, H. Zhao, Performance analysis and optimization of the rough-contact Bi₂Te₃-based thermoelectric cooler via metallized layers, *Case Stud. Therm. Eng.* 40 (2022), 102522.
- [8] S.B. Riffat, G. Qiu, Comparative investigation of thermoelectric air-conditioners versus vapour compression and absorption air-conditioners, *Appl. Therm. Eng.* 24 (14) (2004) 1979–1993.
- [9] C.J.L. Hermes, J.R. Barbosa, Thermodynamic comparison of Peltier, Stirling, and vapor compression portable coolers, *Appl. Energy* 91 (1) (2012) 51–58.
- [10] T. Gong, Y. Wu, L. Gao, L. Zhang, J.T. Li, T. Ming, Thermo-mechanical analysis on a compact thermoelectric cooler, *Energy* (2019) 1211–1224.
- [11] A. Elghool, F. Basrawi, T.K. Ibrahim, K. Habib, H. Ibrahim, D.M.N.D. Idris, A review on heat sink for thermo-electric power generation: Classifications and parameters affecting performance, *Energy Convers. Manag.* 134 (2017) 260–277.
- [12] D. Ji, Z. Wei, J. Pou, S. Mazzone, S. Rajoo, A. Romagnoli, Geometry optimization of thermoelectric modules: Simulation and experimental study, *Energy Convers. Manag.* 195 (2019) 236–243.
- [13] S. Manikandan, S.C. Kaushik, Energy and exergy analysis of an annular thermoelectric cooler, *Energy Convers. Manag.* 106 (2015) 804–814.
- [14] T.H. Wang, Q.H. Wang, C. Leng, X.D. Wang, Parametric analysis and optimal design for two-stage thermoelectric cooler, *Appl. Energy* 154 (2015) 1–12.
- [15] S. Manikandan, S.C. Kaushik, Transient thermal behavior of annular thermoelectric cooling system, *J. Electron. Mater.* 46 (5) (2017) 2560–2569.
- [16] M.E. Kiziroglou, I. Elefantiotis, S. Wright, T. Toh, P.D. Mitcheson, T. Becker, E. Yeatman, Performance of Phase Change Materials for Heat Storage Thermoelectric Harvesting, *Appl. Phys. Lett.* 103 (2013), 193902, 193902.
- [17] G. Tan, D. Zhao, Study of a thermoelectric space cooling system integrated with phase change material, *Appl. Therm. Eng.* 86 (2015) 187–198.
- [18] X. Li, S. Mahmoud, R.K. Al-Dadah, A. Elsayed, Thermoelectric cooling device integrated with PCM heat storage for MS patients, *Energy Procedia* 61 (2014) 2399–2402.
- [19] S. Manikandan, C. Selvam, P. Pavan Sai Praful, R. Lamba, S.C. Kaushik, D. Zhao, R. Yang, A novel technique to enhance thermal performance of a thermoelectric cooler using phase-change materials, *J. Therm. Anal. Calorim.* 140 (3) (2019) 1003–1014.
- [20] X. Wang, J. Xu, F. Zhang, S. Du, Phase change materials at the cold/hot sides of thermoelectric cooler for temperature control, *Proc. SPIE Int. Soc. Opt. Eng.* 6423 (2007), 642318.
- [21] P.E. Ruiz-Ortega, M.A. Olivares-Robles, O.Y. Enciso-Montes De Oca, Supercooling in a new two-stage thermoelectric cooler design with phase change material and Thomson effect, *Energy Convers. Manage.* 243 (2021), 114355.

- [22] A.R.M. Siddique, S. Mahmud, B.V. Heyst, A comprehensive review on a passive (phase change materials) and an active (thermoelectric cooler) battery thermal management system and their limitations, *J. Power Sources* 401 (2018) 224–237.
- [23] R. Bhuiya, N. Shah, D. Arora, N.V. Krishna, S. Manikandan, C. Selvam, R. Lamba, Thermal management of phase change material integrated thermoelectric cooler with different heat sink geometries, *J. Energy Storage* 51 (2022), 104304.
- [24] Y. Cai, B.H. Hong, W.X. Wu, W.W. Wang, F.Y. Zhao, Active cooling performance of a PCM-based thermoelectric device: dynamic characteristics and parametric investigations, *Energy* 254 (2022), 124356.
- [25] W. He, J. Zhou, J. Hou, C. Chen, J. Ji, Theoretical and experimental investigation on a thermoelectric cooling and heating system driven by solar, *Appl. Energy* 107 (2013) 89–97.
- [26] H. Lv, X.D. Wang, T.H. Wang, C.H. Cheng, Improvement of transient supercooling of thermoelectric coolers through variable semiconductor cross-section, *Appl. Energy* 164 (2016) 501–508.
- [27] M. Ma, J. Yu, Experimental study on transient cooling characteristics of a realistic thermoelectric module under a current pulse operation, *Energy Convers. Manag.* 126 (2016) 210–216.
- [28] H. Lv, X.D. Wang, T.H. Wang, J.H. Meng, Optimal pulse current shape for transient supercooling of thermoelectric cooler, *Energy* 83 (2015) 788–796.
- [29] S. Lin, M. Ma, J. Wang, J. Yu, Experiment investigation of a two-stage thermoelectric cooler under current pulse operation, *Appl. Energy* 180 (2016) 628–636.
- [30] X. Liao, Y. Liu, J. Ren, L. Guan, X. Sang, B. Wang, H. Zhang, Q. Wang, T. Ma, Investigation of a double-PCM-based thermoelectric energy-harvesting device using temperature fluctuations in an ambient environment, *Energy* 202 (2020), 117724.
- [31] T. Gong, L. Gao, Y. Wu, H. Tan, F. Qin, T. Ming, J. Li, Transient thermal stress analysis of a thermoelectric cooler under pulsed thermal loading, *Appl. Therm. Eng.* 162 (2019), 114240.



Yuying Yan is a professor of thermofluids engineering at University of Nottingham, UK. He obtained BSc from Jilin University of Technology (January 1982), MSc from Shanghai Institute of Mechanical Engineering (May 1986), and PhD from City, University of London (April 1996). After taking research & academic positions at University of Surrey and Nottingham Trent University, respectively, he joined University of Nottingham in 2004 and was promoted to full Professor as Chair in Thermal Fluids Engineering since 2011. With more than 30-year experience, his research covers widely range area of flow and heat transfer including heat transfer enhancement, phase changes, surface wetting, and nature inspired solutions for energy efficiency, as well as thermoelectric, energy storage and thermal management for electrical and energy systems.



Yong Ren is an Associate Professor in the Department of Mechanical, Materials and Manufacturing Engineering, University of Nottingham Ningbo China. He obtained his PhD degree in mechanical engineering at Hong Kong Polytechnic University. He had worked as a research assistant at the Hong Kong Polytechnic University and as a postdoctoral research associate at the University of Hong Kong. He has a broad range of research interests, including microscale fluid dynamics, heat transfer, computational fluid dynamics modeling, multiphase flow, microfabrication, biomaterial synthesis, and biomedical applications using droplet microfluidics and centrifugal microfluidics.



Jing Wang is an Assistant Professor in the Department of Electrical and Electronic Engineering, University of Nottingham Ningbo China. She obtained her PhD degree in electrical engineering at the University of Nottingham (UK). Her research interests include biosensing technologies and microfluidics techniques.



Xinyu Zhang is an assistant professor in the Department of Mechanical, Materials and Manufacturing Engineering, University of Nottingham Ningbo China. He obtained his PhD degree in mechanical engineering at Clarkson University, USA. His research interests focus on modeling and CFD in multiphase flows, particulate flows and coupled fluid flows, computational combustion and reacting flows, particle technology and particle effects, aerosol dynamics as well as particle transport, deposition and removal, energy systems and renewable/clean energy.



Yanhong Guo is now a PhD student in University of Nottingham Ningbo China. She received her bachelor degree in Department of Physics and Electronic Information, Shangqiu Normal University and master degree in Department of Physics, Lanzhou University. Her research focuses on phase change materials and thermoelectric device